



Aluminium–steel lap joining by multipass friction stir welding



C. Leitao ^{a,*}, E. Arruti ^b, E. Aldanondo ^b, D.M. Rodrigues ^{c,a}

^a CEMUC, Department of Mechanical Engineering, University of Coimbra, Portugal

^b IK4 LORTEK, Ordizia, Gipuzkoa, Spain

^c ISISE, Department of Mechanical Engineering, University of Coimbra, Portugal

ARTICLE INFO

Article history:

Received 2 May 2016

Received in revised form 25 May 2016

Accepted 26 May 2016

Available online 27 May 2016

Keywords:

Multipass welding

FSW

Dissimilar joining

Aluminium

Steel

Bonding mechanisms

ABSTRACT

The use of a multipass welding strategy for increasing the bonding area in the dissimilar friction stir lap welding (FSLW) of aluminium to steel is analysed in current work. In order to minimize tool wear, the pin penetration into the lower plate, the steel plate, was set to a minimum. By performing partially overlapped welding passes it was possible to analyse the quality of the bonding across the multipass weld. The microstructural analysis of the bonding interface, after weld collapse in tensile-shear testing, enabled to conclude that by minimizing the pin penetration in the steel plate, the formation of intermetallics in the bonding interface is suppressed and base materials joining results from mechanical bonding and solid state solution. However, for each welding pass, the bonding is not uniform/continuous across the pin trajectory. The deleterious effect of the bonding discontinuities on the monotonic weld strength may be limited by overlapping the successive weld passes, in order to maximize the bonding area. Improving the fatigue strength requires optimizing the welding parameters and/or pin positioning relative to the lower plate in order to avoid the occurrence of micro-cavities at the bonding interface.

© 2016 Elsevier Ltd. All rights reserved.

1. Introduction

Due to its relevance for engineering applications, mainly in the transportation industry, the lap joining of Aluminium to Steel (Al–Fe) become one of the most important topics in dissimilar Friction Stir Lap Welding (FSLW) research and development. Since 2004, several works were published in this field, encompassing a wide range of different steels and aluminium alloys combinations, as it is possible to depict from Fig. 1, where the works already performed are displayed and the base materials addressed by each one identified. In spite of the diversity in base materials combinations addressed in the literature, it looks well-accepted that the aluminium plate, i.e., the softer base material of the combination, must be always placed on the top of the joint in order to reduce tool wear during welding.

The common objective of most of the works cited in Fig. 1 was the characterization of the microstructural bonding mechanisms taking place during welding. Elrefaey et al. [1] argue that the Al–Fe bonding is promoted by a layered structure formed in a steel fine-grained zone, adjacent to the base materials interface, and constituted by Fe₂Al₅ and Fe₄Al₁₃ intermetallic compounds (IMC). Other IMC compounds, such as FeAl₃ and FeAl, were also detected by Shen et al. [6] and Kimapong and Watanabe [8], in welds performed with other base materials combinations. Those authors assumed that the presence of a IMC layer is the main bonding mechanism in Al–Fe lap welding. The thickness of

the IMC layer was also found to have an important influence on the welds strength. Lee et al. [13], in Friction Stir Spot Welding (FSSW), established an upper limit of 2 μm for the thickness of the IMC layer, in order to avoid weld strength deterioration.

The relationship between welding parameters, IMC layer morphology and welds strength was also analysed by some authors. Das et al. [10] demonstrated the strong influence of the FSLW thermal cycle on IMC formation, concluding that the higher the heat registered during the process, the larger the IMC layer. Complementarily, Kimapong and Watanabe [7,8] reported that the formation of FeAl₃ brittle IMC can be avoided by increasing the weld speed and decreasing the tool rotation speed, i.e., lowering the heat generation and increasing the heating and cooling rates. Finally, according to Ogura et al. [5], the nature of the IMC formed during welding is determined by the combined influence of base materials stirring and thermal conditions.

Beyond the IMC layer, other Al–Fe bonding mechanisms were already reported in dissimilar FSLW literature. Da Silva et al. [3] determined that a mechanical interlocking effect and diffusion bonding between the aluminium sheet and the Al–Si coating of a 22MnB5 steel were the main bonding mechanisms in AA1050–22MnB5 dissimilar Al–Fe joining. According to Chen and Nakata [14], the surface finish of the steel plate may influence the type of bonding mechanisms in FSLW of aluminium to steel. The authors analysed Al–Fe welds produced using a zinc-coated steel, a brushed finish steel and a mirror finish steel, and depicted differences between the bonding mechanisms for the three steel types. For the weld performed with the galvanized steel, the authors realized that the bonding between the plates was promoted

* Corresponding author.

E-mail address: carlos.leitao@dem.uc.pt (C. Leitao).

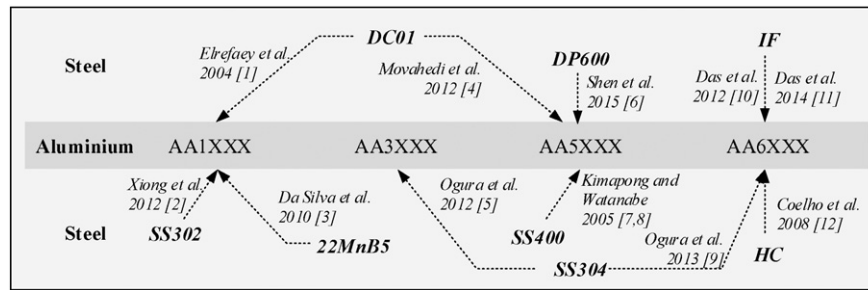


Fig. 1. Base material combinations in the literature on aluminium-steel FSLW.

by a multi-layer structure constituted by IMCs, zinc and iron. On the other hand, for the weld produced with the brushed finish steel, i.e., the one with the rougher surface, it was found that the aluminium was pushed into the cavities in the steel surface, promoting mechanical bonding between the two base materials. These findings proved that the Al–Fe bonding can be obtained by joining mechanisms other than the formation of a IMC layer.

Being intrinsically related with base materials stirring, the influence of the pin plunge depth on the bonding mechanisms was also addressed in the cited literature. According to Shen et al. [6] as well as Da Silva et al. [3], the use of different pin plunge depths influences the bonding. In addition, the use of an excessive plunge depth was harmful due to the intense pin wear, caused by the tool penetration into the steel plate. Kimapong and Watanabe [7,8] found that by increasing the plunge depth, the thickness of the IMC layer was increased, leading to a decrease of the weld strength. In this way, it is possible to conclude that, in Fe–Al FSLW, it is required to set an optimum tool plunge depth, enabling to minimize the pin penetration into the steel plate and, simultaneously, to promote the bonding between the two plates. Ogura et al. [9] found that minimizing the pin plunge depth, only 62% of the area along the rotating tool path could be regarded as bonded, which was detrimental in terms of weld strength.

From the cited literature it can be concluded that maximizing the bonded area and minimizing the pin plunge depth is the most interesting solution in order to produce Al–Fe welds with improved strength at minimum tool costs. The main propose of this work is to provide an insight discussion on the best strategies to achieve this objective by performing multipass welding.

2. Experimental procedure

Multipass lap-welds were fabricated using 3 and 5 mm thick plates of the AA6082-T6 aluminium alloy and S355J2 + N steel, respectively. All the welds were performed in load control using an MTS I-STIR PDS equipment, at LORTEK facilities, in Spain, and the welding parameters described in Table 1. As mentioned in the introduction, the multipass welding strategy, schematically shown in Fig. 2, was planned in order to increase the bonding area between the two base material plates. At the same time, both the axial load (F_z) and pin length (l_p) were selected in order to minimize the pin penetration into the lower plate and, in this way, to minimize tool wear. The tool shoulder, which worked in contact with the Al plate, was made from M42 steel and the pin, which should work in contact with the steel plate, was made from WC-Co non-threaded cylindrical rod material of 4 mm in diameter.

Transverse cross-section specimens of the weld were cut for metallographic analysis, cold mounted, polished, chemically etched with modified Poulton's and Nital 3% reagents, and observed using a Zeiss

Table 1
FSLW parameters.

v (mm/min)	ω (rpm)	α (deg.)	F_z (kN)	\varnothing_s (mm)	\varnothing_p (mm)	l_p (mm)
305	800	1.5	8.8	12	4	3.1

Stemi 2000-C and Leica DM4000 M LED microscopes. Scanning electron microscopy with Energy dispersive X-Ray spectrometry (SEM/EDS) and X-Ray diffraction were performed in the interface of the welds, using a PHILIPS XL30 SE microscope and a PANalytical XPert PRO micro diffractometer, respectively. An ALICONA Infinite Focus (IFM) 3D microscope was used in order to register the topography of the weld interfaces. The mechanical heterogeneity across the different weld zones was assessed by performing several hardness measurements along the weld width and thickness, using a Struers Duramin equipment with a load of 200 gf applied for 15 s. The local tensile properties of the different weld zones were assessed by performing tensile tests of upper weld plate samples (see Fig. 3a) and using the hardness results in the relationships developed in [15]. GOM Aramis 5M System was used for strain data acquisition by Digital Image Correlation (DIC) during the tensile tests. All the procedures adopted for stress-strain data analysis are explained in [16,17].

The weld strength was evaluated in monotonic and cyclic loading conditions by performing shear-tensile tests (see Fig. 3b). Due to the specific configuration of the joint, only the advancing side of the weld was tested. The monotonic loading tests were performed in a 100 kN universal testing machine (Instron 4206). Three lap-weld samples were tested in order to confirm the reproducibility of the results. The weld response to cyclic loading was obtained by performing fatigue tests, using an Instron ElectroPlus E10000 machine, with a frequency of 10 Hz, a stress ratio set to $R = 0.01$ and stress ranges between 30 and 90 MPa. The load amplitude and mean load were calculated taking into account the values of the stress ranges, the thickness of the thinnest base material, the width of the specimens and the stress ratio. Fatigue results were represented as $S-N$ curves, where the stress range vs. the

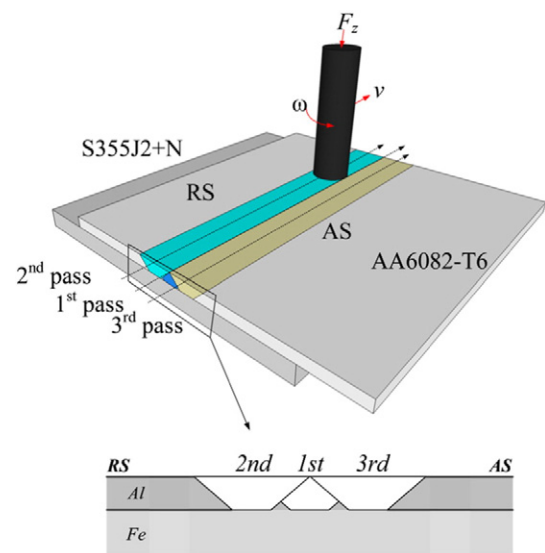


Fig. 2. Scheme of welds fabrication procedure.

Download English Version:

<https://daneshyari.com/en/article/827875>

Download Persian Version:

<https://daneshyari.com/article/827875>

[Daneshyari.com](https://daneshyari.com)